Breakup of the projectile at 35 MeV/nucleon

P. L. Gonthier, P. Harper, B. Bouma, and R. Ramaker
Department of Physics, Hope College, Holland, Michigan 49423

D.A. Cebra, Z.M. Koenig, D. Fox,* and G.D. Westfall
National Superconducting Cyclotron Laboratory and Department of Physics and Astronomy, Michigan State University, East Lansing, Michigan 48824

(Received 15 December 1989)

Projectile breakup processes are probed by studying the emission of α particles in coincidence with projectile-like fragments as a function of the dissipated energy in the collisions of 35 MeV/nucleon ^{16}O with ^{58}Ni. Energy correlations between α particles and projectile-like fragments at small-angle geometries allow the separation of the sources of α emission from projectile-like and target-like fragments. We find that the slope parameters of the decay energy distributions, the average excitation energies, and the α particle multiplicities of the projectile-like fragments increase with increasing dissipation of energy. If the linear dependence, exhibited by the data, of the slope parameter with the dissipated energy is included in model calculations, the majority of the coincidence yield in the forward hemisphere can be explained. However, an excess yield of the data on the opposite side of the beam from the observed projectile-like fragment still remains. Such analysis of the data suggests that the breakup of the projectile is the dominant source of light particles at forward angles. Processes resulting in the breakup of the projectile must be better understood in order to study other processes leading to similar phenomena.

I. INTRODUCTION

The role of sequential decay processes in heavy ion reactions from 4 to 20 MeV/nucleon has been explored in several studies[1-11] where light charged particles are measured in coincidence with projectile-like fragments (PLF's). In this energy region, most of the light particles are emitted sequentially by the PLF's. Sequential emission is the decay of statistically equilibrated PLF's and target-like fragments (TLF's) that have been fully accelerated by the Coulomb field of the two interacting nuclei. However, some studies suggest the importance of processes occurring on a time scale faster than sequential decay processes. There are indications[1,3-6,9,11] for fragmentation-like processes where α particles are emitted during the early stages of the collision after which the PLF undergoes a damped reaction with the target. These reactions have been referred to as uncorrelated,[5,6] incoherent breakup,[4] and quasibreakup[3] processes resulting in the prompt emission of α particles. In this paper we will address the nature of the decay of PLF's at 35 MeV/nucleon and focus on the degree to which breakup processes contribute to the production of light charged particles in the forward direction. We use the term "breakup" in a general sense describing the decay of the excited projectile without reference to any particular decay mechanism. Specifically, we observe that breakup processes of the projectile are a significant source of light particles accounting for the major fraction of the coincidence yield in the forward hemisphere.

II. EXPERIMENTS

We performed an experiment[12] using 35 MeV/nucleon ^{16}O projectiles accelerated at the National Superconducting Cyclotron Laboratory to irradiate an 850 μg/cm^2 target of enriched ^{58}Ni. Alpha particles were detected in 8 telescopes located at 15°, 30°, 45°, 60°, 75°, 90°, 113°, and 135° with respect to the incident beam. The four most forward α-particle telescopes consisted of Si ΔE surface barrier detectors (90 and 150 μm) backed by 10-cm NaI(Tl) detectors, while the backward telescopes consisted of Si ΔE (20 to 35 μm) and 5-mm Si(Li) E detectors. PLF's of Z = 3–8 were detected in two telescopes made up of 100 μm ΔE Si backed by 5-mm Si(Li) detectors and located at 10° relative to the incident beam. In this paper we refer to angles of the α particle telescopes on the same side of the beam as the detected PLF's with a positive sign and on the opposite side with a negative sign.

III. EXPERIMENTAL RESULTS

A. Energy correlations

The clearest manifestation of the sequential breakup of the projectile occurs at small opening angles between the PLF telescope and the α telescope. This geometry allows, in part, the decomposition of the coincidence yield from the emission of α particles from the PLF's and TLF's. In this experiment the PLF's were detected at θ_{PLF}

 ©1990 The American Physical Society

= +10°, and the closest angle to the PLF's at which α particles were observed was at $\theta_\alpha = +15°$ on the same side of the beam as the observed PLF's. The signature for the sequential decay of PLF's has been seen best in the energy correlation of the α particles observed close to the PLF's. A plot of the laboratory energy of the α particles E_α vs the laboratory energy of the carbon ions E_C is displayed in Fig. 1 for α particles at the indicated angles in coincidence with carbon. The data at $\theta_\alpha = +15°$ reveal a pattern of two high intensity regions with a pronounced valley between them. These two lobes are typical of the sequential decay of the PLF's some of which have been reported previously in studies of the α particle decay of ^{16}O in the following reactions:

4 MeV/nucleon ^{16}O with ^{27}Al,[2]

^{14}N in the reactions of 7 MeV/nucleon ^{14}N with ^{27}Al,[3]

^{10,11}B and ^{6,7}Li in the reactions of 10 MeV/nucleon ^{14}N with ^{159}Tb,[5]

^{16}O in the reactions of 15 MeV/nucleon ^{14}N with ^{93}Nb,[9]

^{20}Ne in the reactions of 13 MeV/nucleon ^{20}Ne with ^{40}Ca,[8]

^{20}Ne and ^{19}F in the reactions of 15 MeV/nucleon ^{20}Ne with ^{197}Au.[7]

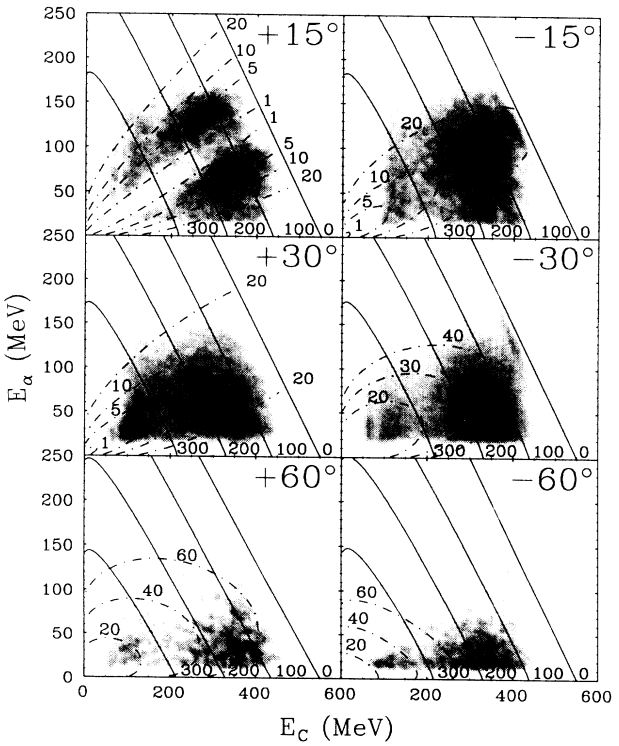

FIG. 1. Density plot, with the intensity varying linearly, for α particles at the indicated angles in coincidence with carbon at $\theta_{PLF} = +10°$. The data have been smoothed using a two-dimensional Gaussian distribution, and gray scaled with 8×8 pixel cells. Curves represent three body kinematic calculations. The dot-dashed curves correspond to various values of the relative energy (MeV) between ^{12}C and α particle assuming the breakup of ^{16}O into ^{12}C + α. The solid curves correspond to the total excitation energy, $-Q_3$ (MeV).

The upper lobe is populated by the forward emission of α particles in the rest frame of the emitting ^{16}O while the recoiling ^{12}C loses energy in the laboratory frame of reference. The lower lobe results from the backward emission of α particles while the recoiling ^{12}C gains energy. Hence the two lobes are formed—one at larger E_α and smaller E_C and the other at smaller E_α and larger E_C. The dot-dashed curves in the Fig. 1 represent various values of the relative energy between the α particle and the ^{12}C assuming the breakup of ^{16}O. The total available excitation energy ($-Q_3$) dissipated in the collision is represented by the solid curves. The highest yield at $\theta_\alpha = +15°$ is observed for events with a relative energy $\approx$4 MeV corresponding to the Coulomb barrier (plus temperature) between an α particle and a ^{12}C and a total excitation energy $\approx$150 MeV. While geometric efficiencies must be considered, the similar yields of both lobes is an indication of a sequential process. This similarity suggests that the lifetime of the excited projectile is long compared to the interaction time. The intensity pattern in Fig. 1 at $\theta_\alpha = +15°$ is very different from the pattern at $\theta_\alpha = -15°$. At $\theta_\alpha = +15°$, which corresponds to an opening angle of 5° with respect to the PLF telescope, there is a kinematic selection of the two solutions. At $\theta_\alpha = -15°$, with an opening angle of 25° with respect to the PLF telescope, the kinematics allow the possibility of two solutions (for example with relative decay energy of 20 MeV). However, the data show only one broad intensity pattern. On both sides of the beam the patterns for all $|\theta_\alpha| \geq 30°$ are very similar.

The distinct pattern of two lobes in Fig. 1 at $\theta_\alpha = +15°$ is a good indication that the α-C coincidences proceed from the single α decay of ^{16}O, and multiple emission is not a major contribution. For multiple emission of two α particles, the ^{16}O picks up an α particle and subsequently decays into two α particles and ^{12}C. If multiple emission were a major factor, the α-C correlation would be less distinct as a smooth background would be added to the yield. Also the α-N coincidence yield is a factor of five smaller that the α-C coincidence yield, suggesting that the pickup channel is not very significant.

In Figs. 2 and 3, we present the intensity plots for the two-dimensional distributions of α particles in coincidence with boron and beryllium, respectively. Kinematic lines of relative energies and total excitation energies are shown in Figs. 2 and 3 assuming the α particle decay of ^{15}N and ^{11}C, respectively. Similar sequential decay patterns are observed at $\theta_\alpha = +15°$. In the case of beryllium in Fig. 3, the most probable relative energies between the α particles and the recoiling beryllium are smaller due to the smaller atomic number of beryllium, and, therefore, the two lobes have merged into one intensity pattern. Most of the yield at $\theta_\alpha = +15°$ in Figs. 1–3 results from the breakup of PLF's. The comparison of Figs. 1–3 reveal similar characteristics associated with the α particle decay of fragments leading to PLF's of $Z = 4 - 6$ indicating that the disassembly of the projectile occurs via an inelastic collision exciting PLF's which later decay in

flight by sequential breakup after the PLF's and TLF's have been fully accelerated away from each other.

In the cases of α-B and α-Be coincidences, we cannot rule out the multiple decay of the projectile as in the case of α-C coincidences. In order to observe B or Be, the excited projectile either emits protons and/or neutrons or transfers some nucleons to the target nucleus. These mechanisms cannot be distinguished from this data. Protons and neutrons could be emitted from the excited projectile first with an α particle emitted in the latter stages of the de-excitation. This would still preserve the distinct features in Figs. 1–3 at $\theta_\alpha = +15°$.

In the case of the decay of ^{16}O at $\theta_\alpha = -15°$ and $-30°$, the intensity distributions of Fig. 1 reveal a pronounced ridge about the $Q_3 = 0$ MeV populated by events where the ^{16}O has undergone quasibreakup leaving the α particle, ^{12}C, and ^{58}Ni approximately in their ground states. This phenomenon is unique for the decay of ^{16}O as it is not present in the cases of α particles in coincidence with boron and beryllium. While the yield for these events is small, it is interesting to study why they occur at angles on the opposite side of the beam from the detected ^{12}C and not on the same side as has been observed in other studies.[2,3,6,7] Such collisions reflect excitation energies of ^{16}O between 25 MeV ($\approx$ 18 MeV relative energy and 7.5 MeV Q value) at $\theta_\alpha = -15°$ and 60 MeV at $\theta_\alpha = -30°$. If these events were to be observed at $\theta_\alpha = +15°$, such high relative energies would require either large or small laboratory energies of carbon and so, fall on the tails of the energy distribution of the primary ^{16}O energy distribution. Therefore for this reaction and geometry such events are not observed at $\theta_\alpha = +15°$ in Fig. 1.

B. Efficiency calculations

In order to understand what bias is introduced by the detector geometries into the coincidence distributions for the breakup of the PLF's in Figs. 1–3, we performed efficiency calculations using the Monte Carlo technique. The resulting distributions are displayed in Fig. 4 for carbon, boron, and beryllium, respectively, in coincidence with α particles detected at +15°. We assumed that the emission of the α particles in the rest frame of the decaying nucleus is isotropic and the energy and angular distributions of the primary PLF's prior to breakup are independent of energy and angle. The efficiency calculations indicate that the close-angle geometry tends to

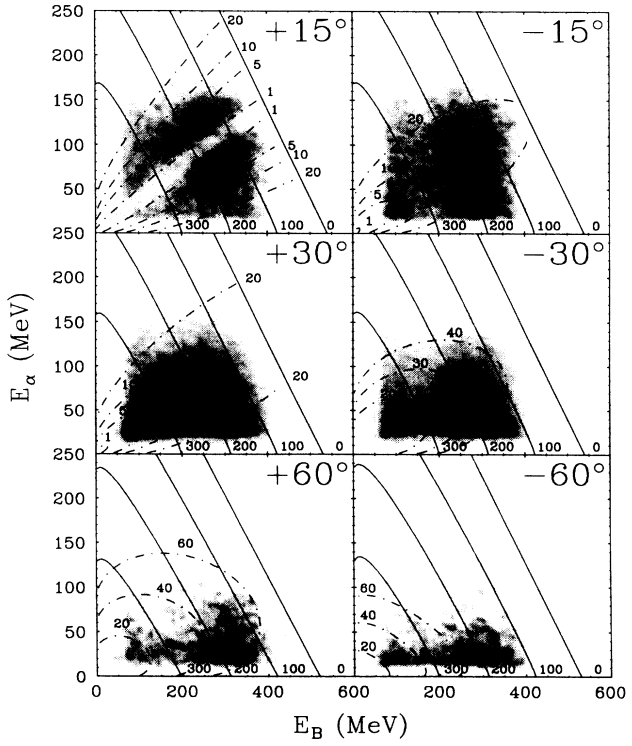

FIG. 2. Density plot, with the intensity varying linearly, for α particles at the indicated angles in coincidence with boron at $\theta_{PLF} = +10°$. The data have been smoothed using a two-dimensional Gaussian distribution, and gray scaled with 8 × 8 pixel cells. Curves represent three body kinematic calculations. The dot-dashed curves correspond to various values of the relative energy (MeV) between ^{11}B and α particle assuming the breakup of ^{15}N into ^{11}B+α. The solid curves correspond to the total excitation energy, $-Q_3$ (MeV).

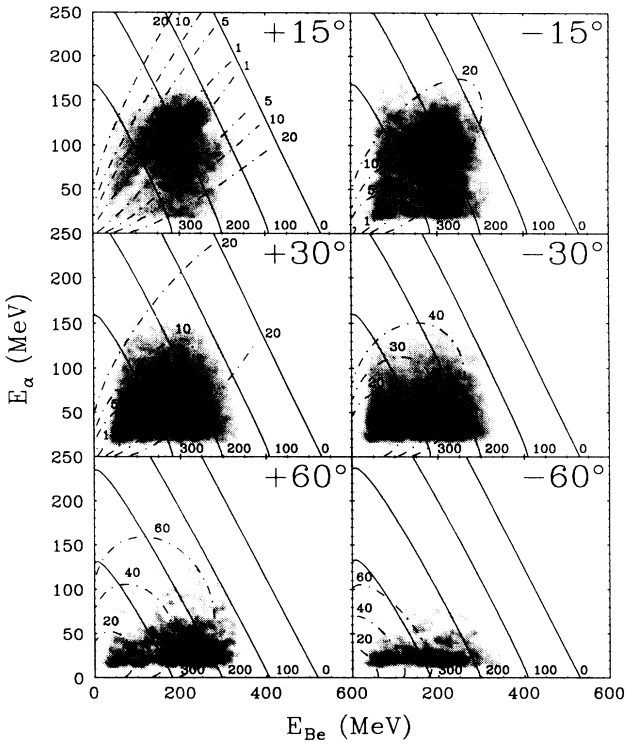

FIG. 3. Density plot, with the intensity varying linearly, for α particles at the indicated angles in coincidence with beryllium at $\theta_{PLF} = +10°$. The data have been smoothed using a two-dimensional Gaussian distribution, and gray scaled with 8 × 8 pixel cells. Curves represent three body kinematic calculations. The dot-dashed curves correspond to various values of the relative energy (MeV) between ^{7}Be and α particle assuming the breakup of ^{11}C into ^{7}Be+α. The solid curves correspond to the total excitation energy, $-Q_3$ (MeV).

enhance events with small relative energies. For example, we present in Fig. 5 spectra of relative energy for the raw data, for the efficiency calculation and for the corrected data for α particles at $\theta_\alpha = +15°$ in coincidence with carbon ions. A window has been placed on the upper lobe in Fig. 1 at $\theta_\alpha = +15°$ to separate α particles coming from the PLF's and TLF's. Alpha particles emitted by TLF's contribute most strongly around the region of $E_\alpha \approx 50$ MeV and $E_{\rm PLF} \approx 30$ MeV/nucleon where a lower lobe exists as seen in Figs. 1–3 for $|\theta_\alpha| \geq 30°$. In order to account for the relevant Jacobian we have randomized the laboratory angle within the solid angle of the respective detectors and randomized the energy within the ADC channel on an event by event basis removing the requirement of multiplying the data by the correct Jacobian.[16] As observed in Fig. 5 the measured distributions of relative energies are too narrow due to this enhancement. We have corrected the data at $\theta_\alpha = +15°$ for this effect by dividing the measured distributions by the calculated ones.

In order to study the effect of the dissipation of the incident energy during the collision, we have made four windows on the primary energy of the excited PLF's. Due to the correction of the yields for geometric effects the distribution of α particles emitted from TLF's are artificially enhanced since the correction is for the decay of PLF's. Recognizing this, we also have placed a window to select only the upper lobe of α particles where the TLF's do not contribute. In Fig. 6, we present the distributions of the decay energies between the α particles at $\theta_\alpha = +15°$ and ^{12}C, ^{11}B, and ^{7}Be at $\theta_{\rm PLF} = +10°$. The energy limits of the windows on the primary energies of the PLF's are indicated in the figures. The dashed curves are results of fitting the experimental distributions with a Maxwellian function of the form

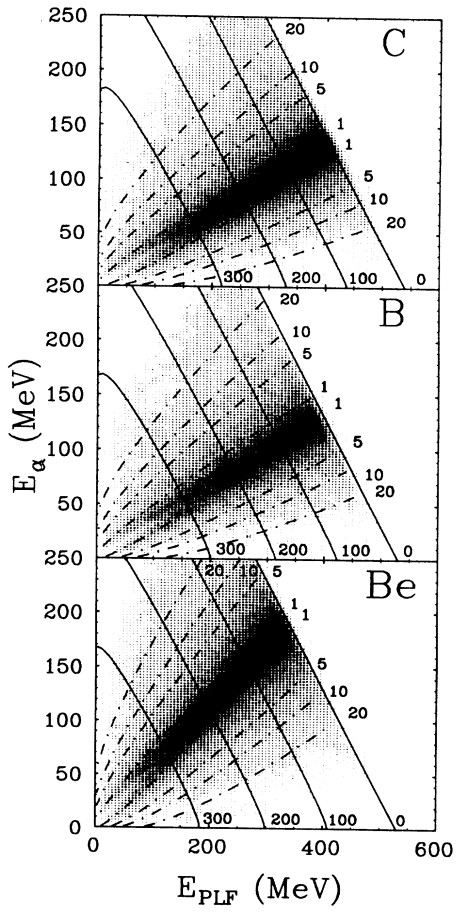

FIG. 4. Density plot, with the intensity varying linearly, of efficiency calculations for α particles at $\theta_\alpha = +15°$ in coincidence with carbon, boron, and beryllium at $\theta_{\rm PLF} = +10°$. The calculated distributions have been smoothed using a two-dimensional Gaussian distribution, and gray scaled with 8×8 pixel cells. Curves represent three body kinematic calculations. The dot-dashed curves correspond to various values of the relative energy (MeV) between the PLF's and α particle. The solid curves correspond to the total excitation energy, $-Q_3$ (MeV).

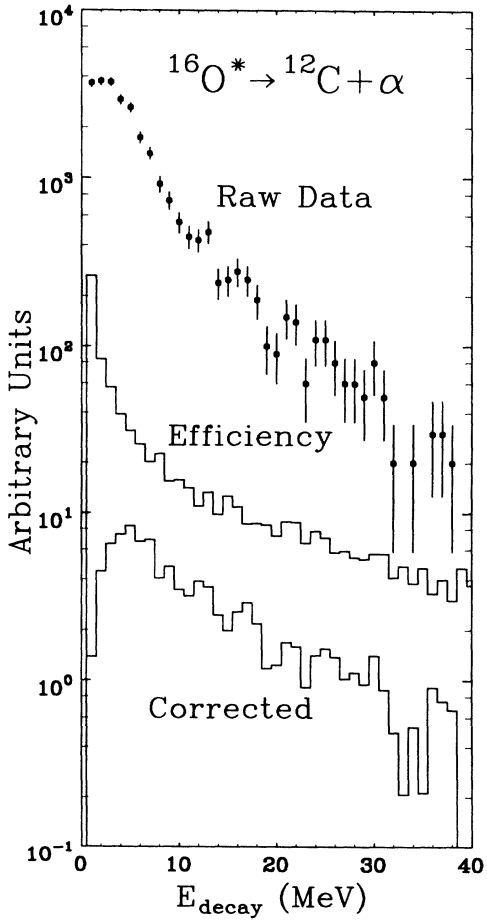

FIG. 5. Energy spectra of the relative energy between α particles at $\theta_\alpha = +15°$ and carbon ions at $\theta_{\rm PLF} = +10°$ assuming the decay of ^{16}O for the experimental data, efficiency calculation, and the corrected data obtained by dividing the raw data by the efficiency calculation.

$$P(E_d) = \text{ const } (E_d - B)e^{-(E_d-B)/T}, \quad (1)$$

where B is the parameter reflecting the Coulomb barrier of the α particle and T is the slope parameter reflecting the apparent temperature of the emitting nucleus. Such a function generally describes the data reasonably well. The barrier parameter remains constant as a function of the PLF energy. However, the slope parameter increases with decreasing primary energy of the PLF's. As more energy is dissipated (smaller primary energy), more excitation energy is available resulting in an increase of the slope parameter or temperature.

C. Slope parameters and excitation energies

We present in Fig. 7 the variation of the slope parameter as a function of the PLF energy windows. The slope parameters are indicated by the solid circles. The dashed line is to guide the eye. In addition, in order to study the emission of α particles from the TLF's, we have fit the α particle energy spectra in the backward hemisphere with a sequential decay model[12] for four similar windows on the laboratory energy of the PLF's. The emission from the TLF's is also parametrized with a Maxwellian function of the same form. The model includes recoil effects due to the variation of the energy of the observed PLF's. We indicate the slope parameters for the TLF's by open diamonds in Fig. 7 with a solid line through the points to guide the eye. The error bars reflect the uncertainties of the fit and the horizontal bars correspond to the standard deviation of the energy distribution of the PLF's for the corresponding windows. The slope parameters have a linear dependence with the exception of the case of the decay of ^{11}C to ^{7}Be+α. The slope parameters for the decay of TLF's remain rather constant showing a small increase with decreasing PLF energy, whereas the slope parameters for the decay of the PLF's show a pronounced increase from 2 to 7 MeV. However, while the slope parameters start out around 2 MeV for high PLF energies, they become very similar to the slope parameter of the TLF for the most dissipative collisions. This result is expected for statistically equilibrated nuclei reaching the

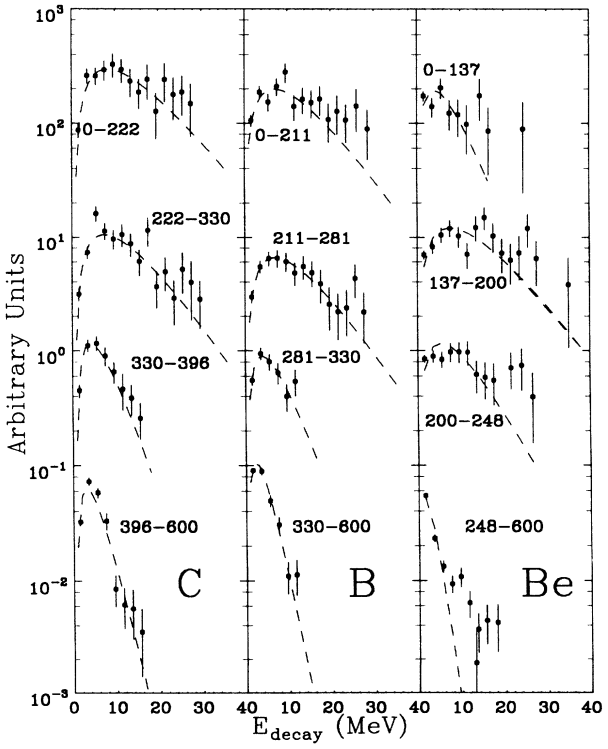

FIG. 6. Energy spectra of the relative energy between α particles at $\theta_\alpha = +15°$ and carbon, boron, and beryllium ions. Spectra are shown for the different windows (limits shown in the figure) on the energy of the primary PLF's. Dashed curves are results of fit to a Maxwellian distribution (see text).

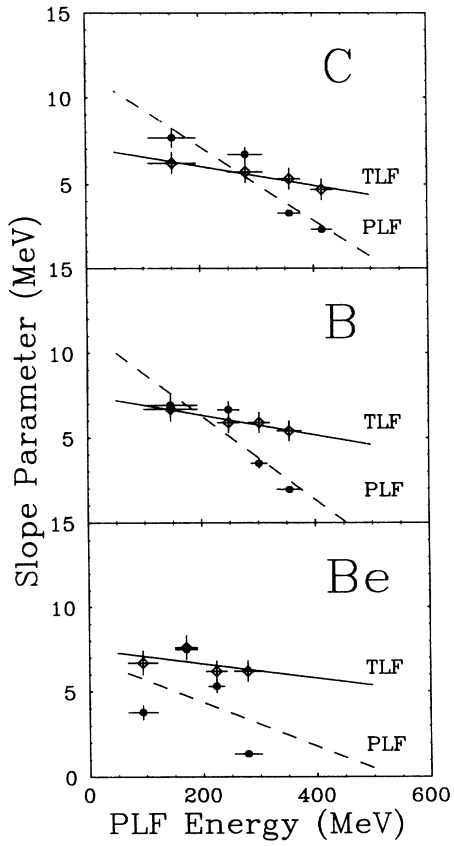

FIG. 7. Slope parameters (PLF) of the relative energy distributions between α particles at $\theta_\alpha = +15°$ and the indicated PLF's at $\theta_{PLF} = +10°$ are plotted (solid dots and dashed lines to guide the eye) as a function of the laboratory energy of PLF's. Slope parameters (TLF) of the relative energy distributions of α particles in coincidence with indicated PLF's at $\theta_{PLF} = +10°$ observed in the backward hemisphere and emitted by TLF's are plotted (open diamonds and solid lines to guide the eye) as a function of the laboratory energy of PLF's. Error bars represent uncertainty of the fits. Horizontal bars represent the standard deviations of the PLF energy in the respective windows.

same temperatures after a sufficiently long interaction time.

At small opening angles, where the observed yield of α particles from the emission of the PLF's is well separated from contribution of the emission of the TLF's, kinematics allows one to make a clear correspondence between the α particle and PLF energies and the energy of the primary fragment (^{16}O, ^{15}N, or ^{11}C) prior to its decay. Assuming that the collision is predominately binary, one can relate the primary fragment energy to the total available excitation energy. In Fig. 8, we plot the average excitation energy of the primary fragment, ^{16}O, ^{15}N, and ^{11}C, as a function of the average total available excitation energy for the four windows on the primary energy of the PLF's mentioned above at $\theta_\alpha = +15°$. The average excitation energies of the primary PLF were extracted from the distributions of relative energies in Fig. 6 plus the Q value of the breakup. The vertical bars in Fig. 8 correspond to the standard deviation of the PLF excitation energies while the horizontal bars correspond to the standard deviation of the total excitation energies within the window on PLF energy. As in the case of the slope parameters in Fig. 7, the average and standard deviation of the excitation energy distributions of the primary PLF's in Fig. 8 increase with increasing available excitation energy. The projectile continues to receive excitation energy as the reaction becomes more violent. The dashed lines indicate the amount of excitation energy of the PLF's if the total excitation energy were shared according to the masses of the two interacting nuclei.

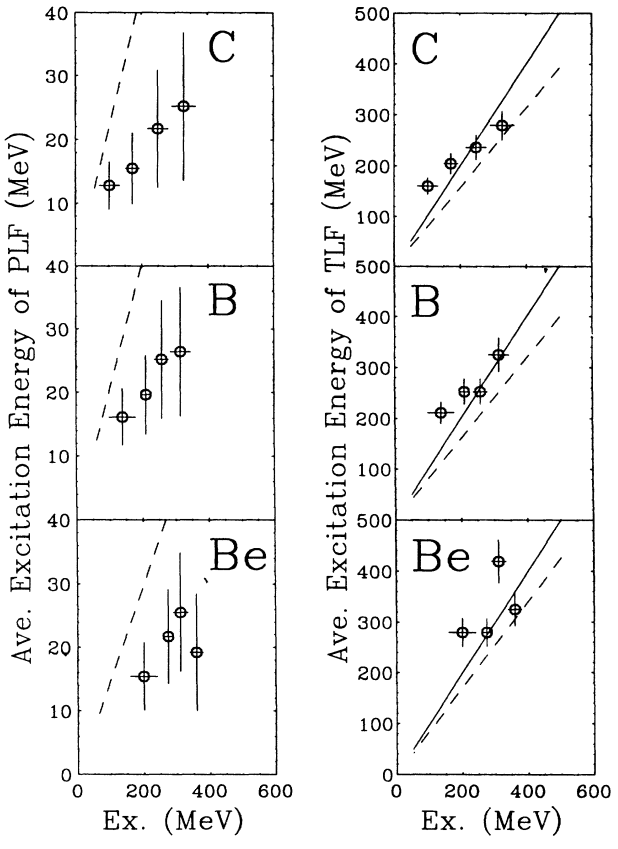

FIG. 8. Average excitation energies of primary PLF's and TLF's are plotted as a function of the average total available excitation energy in the collisions. Dashed lines indicate the expected excitation energies in primary PLF's and TLF's if the total available excitation energy divides according to the masses of the primary interacting nuclei (see text). The solid lines represent the excitation energy of the TLF's if they received all available excitation energy.

If the data measured at small opening angles reflect the general characteristics of the dissipation of energy in these collisions, then the correspondence between the energy of the detected PLF and the total available excitation energy made above may hold true for any α particle detection angle. Obviously, this relationship depends on the opening angle between the detection of the PLF and the α particle. However, if the α multiplicity of the PLF's is around unity, and the data have been corrected for geometric effects, one might expect that the correspondence may still be valid on the average. From the α particle energy spectra in the backward hemisphere, we can relate the excitation energy of the TLF's to the total available excitation energy. Using the formula $E_x = aT^2$, with $a = A/8$, we extract the TLF excitation energies from the slope parameters of the backward angle energy spectra shown in Fig. 7. We present these average excitation energies of the TLF's also in Fig. 8 as a function of the average total available excitation energy for the four windows on the laboratory energies of the PLF's. The dashed lines in Fig. 8 represent the excitation energy of the PLF's and TLF's expected if the total excitation energy divides according to the masses. For primary PLF's the average excitation energies are considerably lower than expected if the excitation energy is divided according to their masses. The data suggest that the TLF's receive larger excitation energies than predicted for the less dissipative collisions but approached the expected values for the most dissipative collisions. The solid lines indicate the excitation energy of the TLF's when they receive the entire available excitation energy. The points above the solid lines are indicative of the uncertainties of the procedure for extracting the excitation energies from the slopes of the α energy spectra at backward angles.

D. Angular correlations

In Fig. 9, we display the angular correlations of α particles in coincidence with carbon, boron, and beryllium ions for the four windows on the energy of the PLF's. The windows on the laboratory energy of the PLF's are indicated in the figure. These windows on the laboratory energy were chosen to have the same limits as the windows on the primary energy of the PLF's previously mentioned in Fig. 7. Here we have placed four windows on the laboratory energy of the PLF's to study the angular correlations as a function of the energy dissipated in the collision. The solid curves are results of model cal-

culations for the sequential decay of the PLF and TLF that include the linear dependence of the slope parameter on the decay of the PLF suggested by the data in Fig. 7. The disagreement occurs with the yield on the opposite side of the beam from the detected PLF where the calculations underestimate the observed yield as also observed in other studies.[1,9,11,12] This increase of the slope parameter with decreasing PLF energy causes the angular correlations to broaden considerably accounting for much of the data at the lower PLF energy windows at the top of Fig. 9. The agreement of the model with the data is best for the most dissipative collisions leading to boron and beryllium. In contrast, the sequential model calculations in the work of Terlau *et al.*[1] for the system 20 MeV/nucleon ^{20}Ne on ^{197}Au agree better with quasielastic events than with deep-inelastic events. In those calculations a common temperature parameter was used, which also remained independent of the energy dissipation. We have allowed the temperature parameter to depend on the dissipated energy. This variation leads directly to broader angular distributions for more damped collisions.

E. Average multiplicities

In order to extract the average α multiplicities, we integrated the angular correlations by assuming symmetry

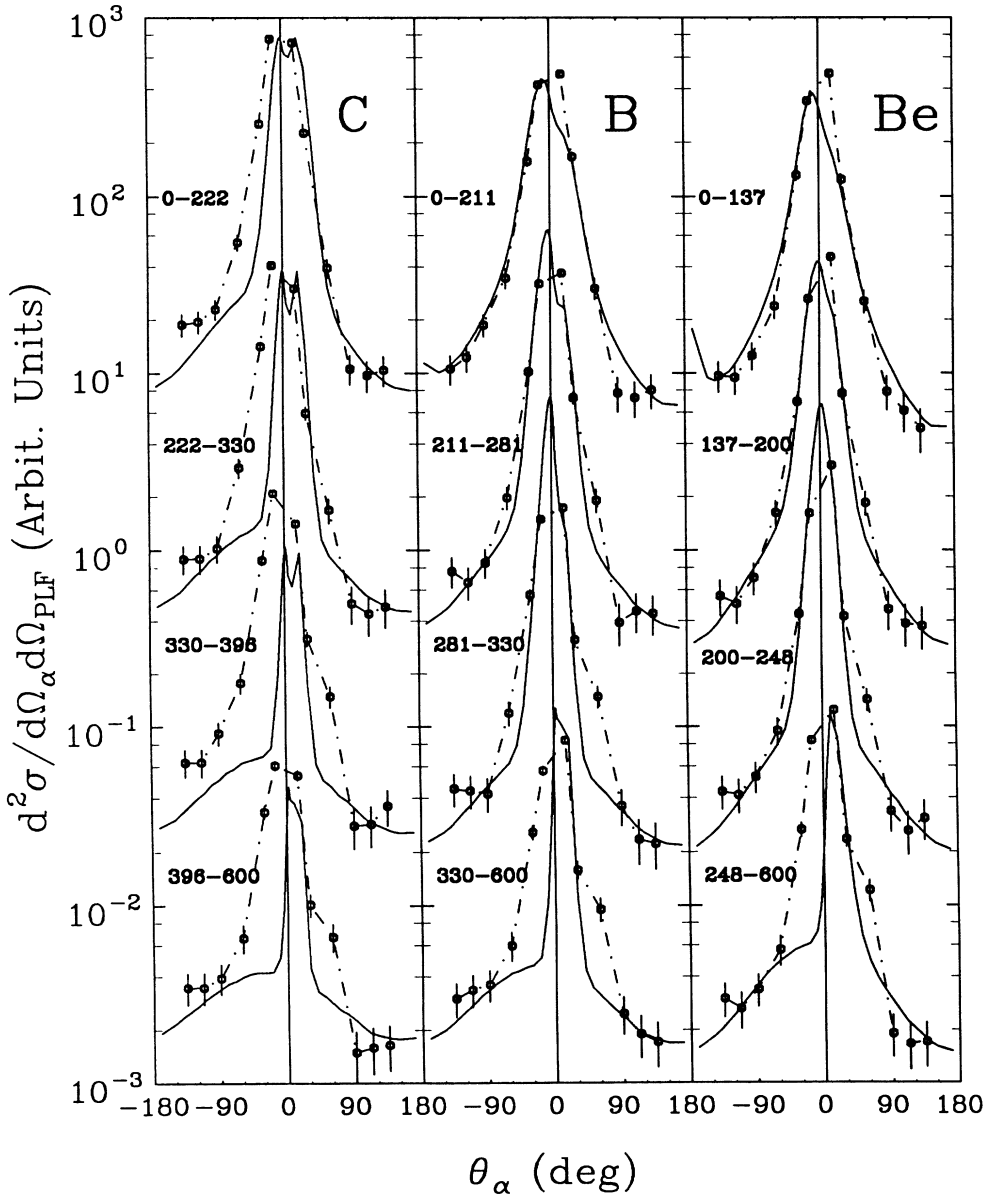

FIG. 9. Angular correlations between α particles in coincidence with indicate PLF's for the different windows (shown in figure) on the laboratory energy of the observed PLF's. Dot-dashed curves join the data points to guide the eye. Solid curves represent the calculations of a sequential model, which includes a slope parameter dependent on the primary energy of the PLF's (see text).

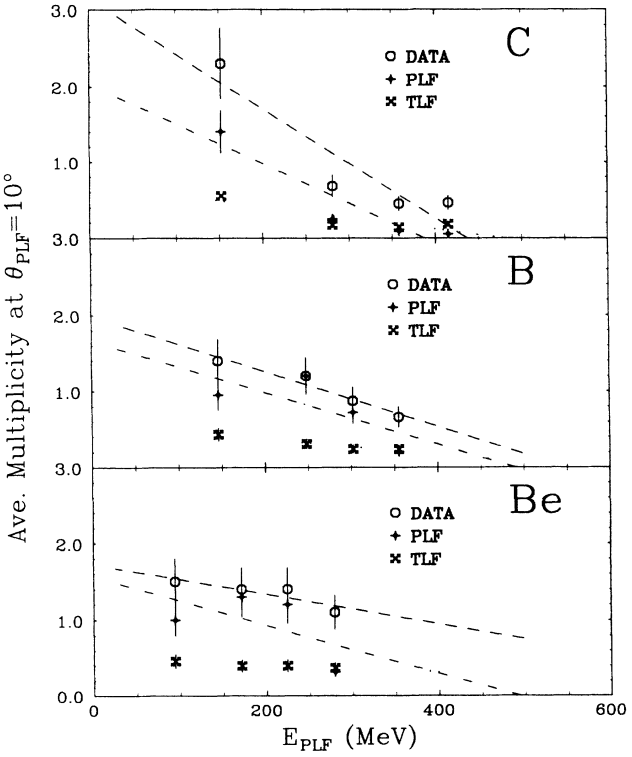

FIG. 10. Average multiplicities of α particles in coincidence with indicated PLF's as a function of the laboratory energy of the observed PLF's. Multiplicities are shown for the experimental data, the contribution from the PLF's and the contribution from the TLF's. Lines guide the eye.

about $\theta = 0°$ in the laboratory frame and divided the coincidence yield by the singles cross section for the respective ion. The average multiplicities as a function of the PLF energy are presented in Fig. 10 for the experimental data, the contribution from the PLF's, and from TLF's calculated by our sequential decay model. The error bars in the figure are estimated uncertainties reflecting the method used to extract the average multiplicities with the limited angular correlations. As expected, the α particle multiplicity increases with increasing energy loss. At large PLF energies (low excitation energies), the α particle multiplicities of the PLF's are comparable to those of the TLF's. The multiplicity for PLF's increases more rapidly than the multiplicity for TLF's as the dissipation of energy increases over the PLF energy region. The data suggest that the greater the availability of the excitation energy the greater the contribution to the yield in the forward direction from breakup processes of the projectile during and after the collision.

The calculations displayed in Fig. 9 model the sequential emission of α particles from the PLF's and TLF's. However, as the dissipation of energy increases the slope parameter increases to 7 or 8 MeV with average excitation energies around 30 MeV for the PLF's. The widths of the levels in ^{16}O, ^{15}N, and ^{11}C become very broad above excitation energies of $\approx$15 MeV. For example, ^{16}O has a level[13] at 25.12 MeV with a width of 3 MeV, ^{15}N has a level[14] at 14.4 MeV with a width of $\approx$1.9 MeV, and ^{11}C has a level[15] at 13.4 MeV with a width of $\approx$1.1 MeV. Such widths lead to lifetimes of the order of 5×10^{-22} s. These lifetimes are shorter that the interaction time of 1×10^{-21} s estimated by the transit time of the projectile across the diameter of the target nucleus. Therefore, if these broad levels are being populated, the PLF's will break up during the interaction leading to α particles in the forward direction with velocities close to the beam. These events do not fall under our category of sequential emission as they would not have isotropic angular distributions in the rest frame of the emitting PLF's and would not be properly simulated by our sequential decay model. What the calculations do indicate is that the sequential and nonsequential breakup of the PLF's may be a significant source of α particles and account for a large fraction of the coincidence yield in the forward hemisphere.

IV. SUMMARY

In conclusion, we have studied the angular and energy correlations of α particles in coincidence with carbon, boron, and beryllium ions produced in the collisions of 35 MeV/nucleon ^{16}O with ^{58}Ni. We observe that the efficiency correction to small angle measurements enhances the decay of PLF's with small relative energies, the efficiency correction leads to a broadening of the decay energy distributions. We find that this broadening increases with increasing available excitation energy because the slope parameters and average excitation energies of the PLF's increase as the damping of the PLF kinetic energy increases. This increase in the excitation energies of the PLF's results in an observed increase in α particle multiplicity. If the linear dependence of the slope parameter of the decay energy distributions of PLF's is included in a sequential decay model, then the majority of the coincidence yield in the forward direction can be accounted for. We recognize that the mechanism is more complicated than pure sequential emission due to the presence of broad levels in PLF's with excitation energies above 15 MeV. These broad levels lead to very short lifetimes that result in the direct breakup of the PLF's during the interaction. Such processes may not have isotropic angular distributions in the emitting frame. However, using the model calculations as a tool to help us interpret the data, we find that the disassembly of the projectile is a major source of light particles in the forward hemisphere. Such breakup processes need to be the identified and separated in order to study other phenomena that also contribute to light particles emitted in the forward hemisphere. Separation of this source may be accomplished in triple (or more) coincidence experiments where the projectile can be reconstructed by detecting its fragments in small angle geometries. Other sources can be studied by measuring other light particles in coincidence with the reconstructed projectile at large opening angles.

ACKNOWLEDGMENTS

We wish to acknowledge the support of the operations crew of the National Superconducting Cyclotron Laboratory. This research was supported by the National Science Foundation under Grant Nos. PHY-8611210 and PHY-8708093 and by a Penta Corporation Grant of Research Corporation.

---

*Present address: Los Alamos National Laboratory, Los Alamos, NM 87545.

[1] W. Terlau, M. Bürgel, A. Budzanowski, H. Fuchs, H. Homeyer, G. Röschert, J. Uckert, and R. Vogel, Z. Phys. A **330**, 303 (1988).

[2] M.B. Tsang, W.G. Lynch, R.J. Puigh, R. Vandenbosch, and A. G. Seamster, Phys. Rev. C **23**, 1560 (1981).

[3] R. Billerey, C. Cerruti, A. Chevarier, N. Chevarier, B. Cheynis, and A. Demeyer, Z. Phys. A **292**, 293 (1979).

[4] W.D. Rae, A.J. Cole, A. Dacal, R. Legrain, B.G. Harvey, J. Mahoney, M.J. Murphy, R.G. Stokstad, and I. Tserruya, Phys. Lett. **105B**, 417 (1981).

[5] R. K. Bhowmik, J. van Driel, R.H. Siemssen, G.J. Balster, P.B. Goldhoorn, S. Gonggrijp, Y. Iwasaki, R.V.F. Janssens, H. Sakai, K. Siwek-Wilczynska, W.A. Sterrenburg, and J. Wilczynski, Nucl. Phys. **A390**, 117 (1982).

[6] J. van Driel, S. Gonggrijp, R.V.F. Janssens, R.H. Siemssen, K. Siwek-Wilczynska, and J. Wilczynski, Phys. Lett. **98B**, 351 (1981).

[7] H. Homeyer, M. Bürgel, M. Clover, Ch. Egelhaaf, H. Fuchs, A. Gamp, D. Kovar, and W. Rauch, Phys. Rev. C **26**, 1335 (1982).

[8] E. Takada, T. Shimoda, N. Takahashi, T. Yamaya, K. Nagatani, T. Udagawa, and T. Tamura, Phys. Rev. C **23**, 772 (1981).

[9] T. Fukuda, M. Ishihara, M. Tanaka, I. Miura, H. Ogata, and H. Kamitsubo, Phys. Rev. C **25**, 2464 (1982).

[10] M. Bini, C.K. Gelbke, D.K. Scott, T.J.M. Symons, P. Doll, D.L. Hendrie, J.L. Laville, J. Mahoney, M.C. Mermaz, C. Olmer, K. Van Bibber, and H.H. Wieman, Phys. Rev. C **22**, 1945 (1980).

[11] P.L. Gonthier, H. Ho, M.N. Namboodiri, J.B. Natowitz, L. Adler, S. Simon, K. Hagel, S. Kniffen, and A. Khodai, Nucl. Phys. **A411**, 289 (1983).

[12] P.L. Gonthier, B. Bouma, P. Harper, R. Ramaker, D.A. Cebra, Z.M. Koenig, D. Fox, and G.D. Westfall, Phys. Rev. C **35**, 1946 (1987).

[13] F. Ajzenberg-Selove, Nucl. Phys. **A460**, 25 (1986).

[14] F. Ajzenberg-Selove, Nucl. Phys. **A449**, 114 (1986).

[15] F. Ajzenberg-Selove, Nucl. Phys. **A433**, 10 (1985).

[16] H. Ho and P.L. Gonthier, Nucl. Instrum. Methods **190**, 75 (1981).

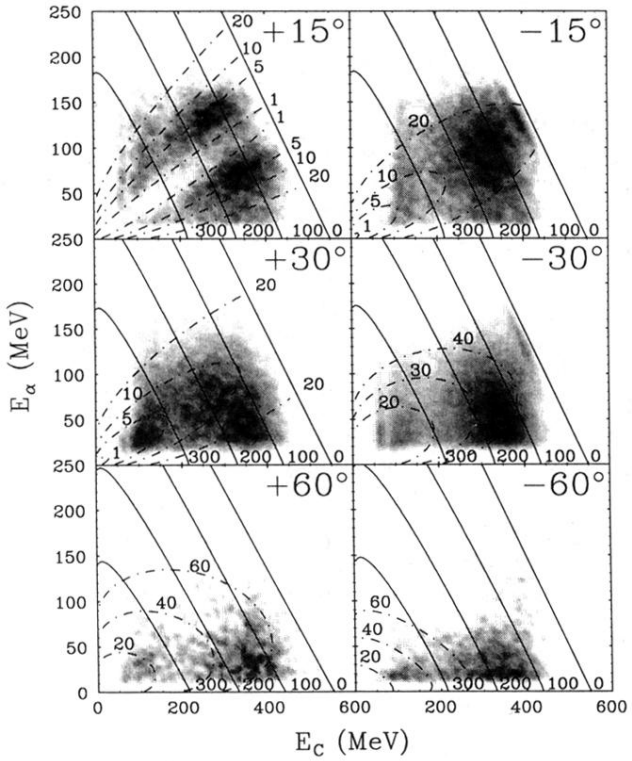

FIG. 1. Density plot, with the intensity varying linearly, for α particles at the indicated angles in coincidence with carbon at $\theta_{\mathrm{PLF}} = +10°$. The data have been smoothed using a two-dimensional Gaussian distribution, and gray scaled with 8×8 pixel cells. Curves represent three body kinematic calculations. The dot-dashed curves correspond to various values of the relative energy (MeV) between ^{12}C and α particle assuming the breakup of ^{16}O into ^{12}C + α. The solid curves correspond to the total excitation energy, $-Q_3$ (MeV).

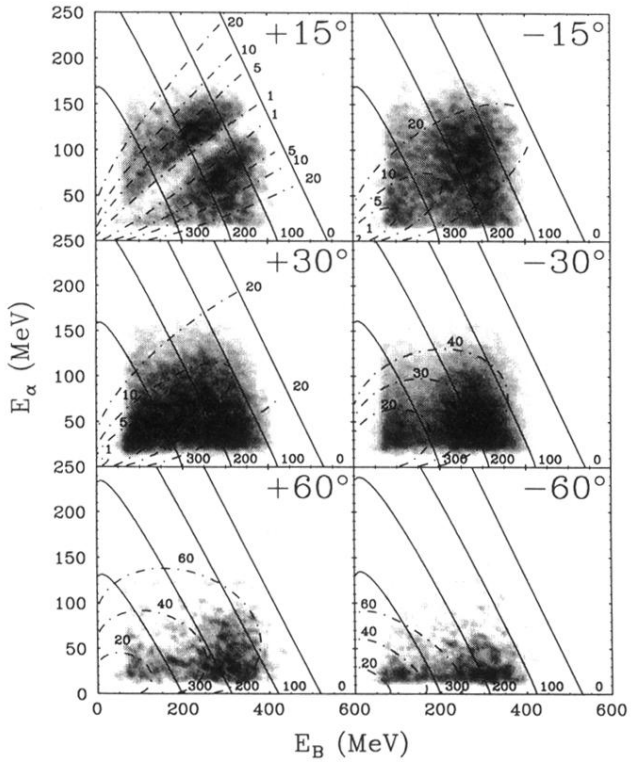

FIG. 2. Density plot, with the intensity varying linearly, for α particles at the indicated angles in coincidence with boron at $\theta_{\rm PLF} = +10°$. The data have been smoothed using a two-dimensional Gaussian distribution, and gray scaled with 8×8 pixel cells. Curves represent three body kinematic calculations. The dot-dashed curves correspond to various values of the relative energy (MeV) between ^{11}B and α particle assuming the breakup of ^{15}N into ^{11}B+α. The solid curves correspond to the total excitation energy, $-Q_3$ (MeV).

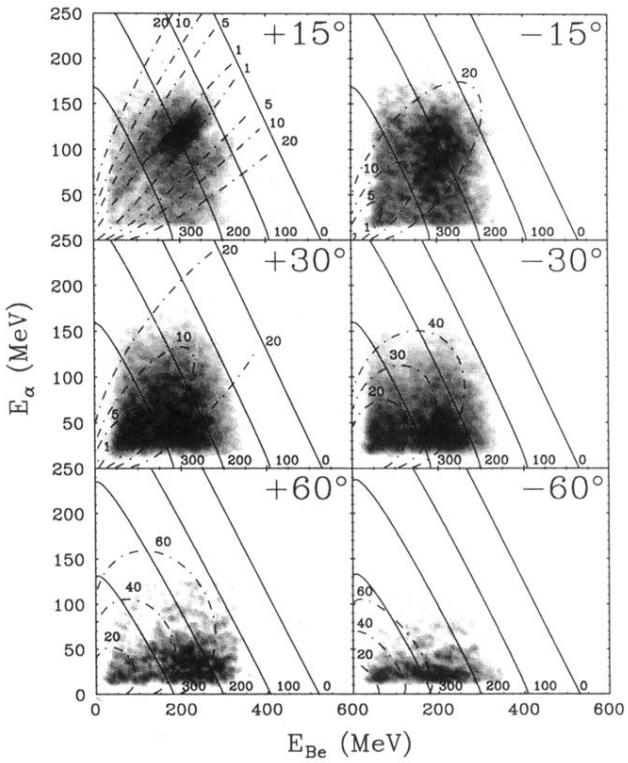

FIG. 3. Density plot, with the intensity varying linearly, for α particles at the indicated angles in coincidence with beryllium at $\theta_{\rm PLF} = +10°$. The data have been smoothed using a two-dimensional Gaussian distribution, and gray scaled with 8×8 pixel cells. Curves represent three body kinematic calculations. The dot-dashed curves correspond to various values of the relative energy (MeV) between ^{7}Be and α particle assuming the breakup of ^{11}C into ^{7}Be+α. The solid curves correspond to the total excitation energy, $-Q_3$ (MeV).

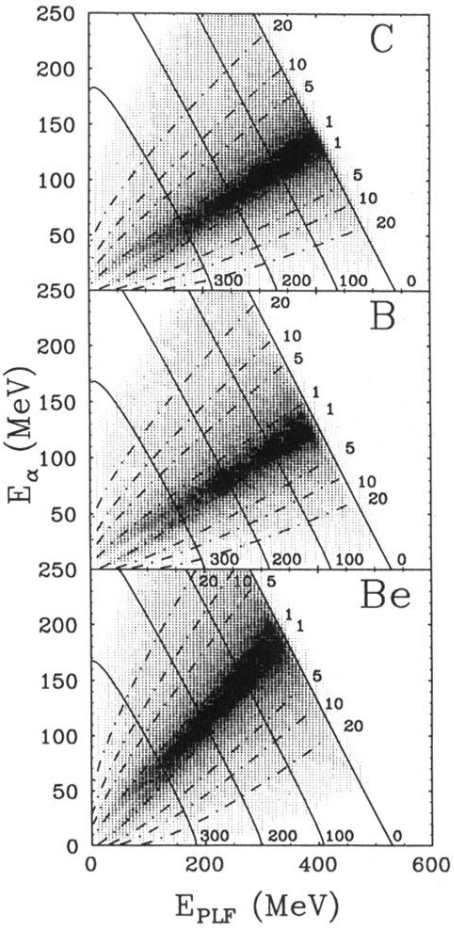

FIG. 4. Density plot, with the intensity varying linearly, of efficiency calculations for α particles at $\theta_\alpha = +15°$ in coincidence with carbon, boron, and beryllium at $\theta_{\rm PLF} = +10°$. The calculated distributions have been smoothed using a two-dimensional Gaussian distribution, and gray scaled with 8×8 pixel cells. Curves represent three body kinematic calculations. The dot-dashed curves correspond to various values of the relative energy (MeV) between the PLF's and α particle. The solid curves correspond to the total excitation energy, $-Q_3$ (MeV).